Delft University of Technology

Room-temperature several-hundred-of-megahertz charge sensing with single-electron resolution using a silicon transistor

Nishiguchi, Katsuhiko; Yamaguchi, Hiroshi; Fujiwara, Akira; Van Der Zant, Herre S.J.; Steele, Gary A.

DOI
10.1063/5.0131808

Publication date
2023

Document Version
Final published version

Published in
Applied Physics Letters

Citation (APA)
Nishiguchi, K., Yamaguchi, H., Fujiwara, A., Van Der Zant, H. S. J., & Steele, G. A. (2023). Room-temperature several-hundred-of-megahertz charge sensing with single-electron resolution using a silicon transistor. *Applied Physics Letters*, *122*(4), Article 043502. https://doi.org/10.1063/5.0131808

Important note
To cite this publication, please use the final published version (if applicable).
Please check the document version above.

Copyright
Other than for strictly personal use, it is not permitted to download, forward or distribute the text or part of it, without the consent of the author(s) and/or copyright holder(s), unless the work is under an open content license such as Creative Commons.

Takedown policy
Please contact us and provide details if you believe this document breaches copyrights.
We will remove access to the work immediately and investigate your claim.

This work is downloaded from Delft University of Technology.
For technical reasons the number of authors shown on this cover page is limited to a maximum of 10.

Green Open Access added to TU Delft Institutional Repository

'You share, we take care!' - Taverne project

https://www.openaccess.nl/en/you-share-we-take-care

Otherwise as indicated in the copyright section: the publisher
is the copyright holder of this work and the author uses the
Dutch legislation to make this work public.

Applied Physics Letters

Room-temperature several-hundred-of-megahertz charge sensing with single-electron resolution using a silicon transistor

Cite as: Appl. Phys. Lett. **122**, 043502 (2023); https://doi.org/10.1063/5.0131808
Submitted: 24 October 2022 • Accepted: 05 January 2023 • Published Online: 23 January 2023

Katsuhiko Nishiguchi, Hiroshi Yamaguchi, Akira Fujiwara, et al.

ARTICLES YOU MAY BE INTERESTED IN

Purcell enhanced single-photon emission from a quantum dot coupled to a truncated Gaussian microcavity
Applied Physics Letters **122**, 043503 (2023); https://doi.org/10.1063/5.0128631

Fidelity of counting the transferred electrons in a GaAs-based monolithic single-electron pump and transistor system with a charge-lock feedback circuit
Applied Physics Letters **122**, 043504 (2023); https://doi.org/10.1063/5.0135114

Enhanced photovoltaic effect in graphene–silicon Schottky junction under mechanical manipulation
Applied Physics Letters **122**, 041102 (2023); https://doi.org/10.1063/5.0128962

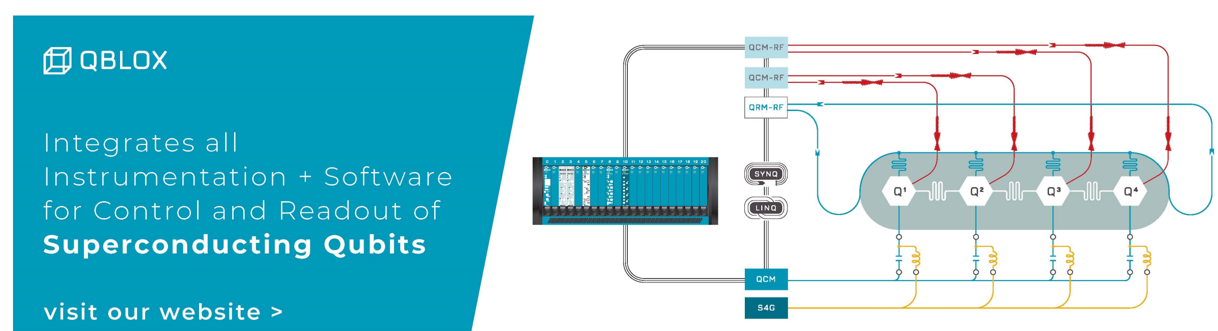

© 2023 Author(s).

Applied Physics Letters ARTICLE scitation.org/journal/apl

Room-temperature several-hundred-of-megahertz charge sensing with single-electron resolution using a silicon transistor

Cite as: Appl. Phys. Lett. **122**, 043502 (2023); doi: 10.1063/5.0131808
Submitted: 24 October 2022 · Accepted: 5 January 2023 ·
Published Online: 23 January 2023

View Online

Export Citation

CrossMark

Katsuhiko Nishiguchi,[1,a)] Hiroshi Yamaguchi,[1] Akira Fujiwara,[1] Herre S. J. van der Zant,[2] and Gary A. Steele[2]

AFFILIATIONS

[1]NTT Basic Research Laboratories, Nippon Telegraph and Telephone Corporation, 3-1 Morinosato Wakamiya, Atsugi, Kanagawa 243-0198, Japan
[2]Kavli Institute of Nanoscience, Delft University of Technology, Lorentzweg 1, 2628 CJ Delft, The Netherlands

[a)]Author to whom correspondence should be addressed: katsuhiko.nishiguchi.vu@hco.ntt.co.jp

ABSTRACT

We demonstrate charge detection with single-electron resolution at high readout frequency using a silicon field-effect transistor (FET) integrated with double resonant circuits. A FET, whose channel of 10-nm width enables a single electron to be detected at room temperature, is connected to resonant circuits composed of coupled inductors and capacitors, and these double resonant circuits provide two resonance frequencies. When the FET is driven by a carrier signal at the lower resonance frequency, a small signal applied to the FET's gate modulates the resonance condition, resulting in a reflected signal appearing near the higher resonance frequency. Such operation utilizing the double resonant circuits enables charge detection with a single-electron resolution of 3×10^{-3} $e/\mathrm{Hz}^{0.5}$ and a readout frequency of 200 MHz at room temperature. In addition, a variable capacitor used in the double resonant circuits allows charge-sensing characteristics to be controlled *in situ*.

Published under an exclusive license by AIP Publishing. https://doi.org/10.1063/5.0131808

Nanometer-scale field-effect transistors (FETs) functioning as a highly sensitive charge sensor can be used to detect not only one electron functioning as a bit of information for data processing[1,2] but also small amounts of charge originating from DNA,[3] photons,[4] and mechanical displacement of nanoelectromechanical systems (NEMSs).[5] In addition, sensors that can detect single electrons have accelerated developments in academic research, including quantum mechanics[6–9] and information thermodynamics.[10–16] On the other hand, the ability to sense a high-speed signal also promises further development and improvement of applications, such as NEMS sensors, detecting extremely small mass[17,18] as well as academic pursuits, such as exploring quantum mechanics.[19] However, since high charge sensitivity of the FET originates from its narrow channel,[20] its channel resistance becomes large, resulting in difficulties in sensing a high-speed signal from the RC rise time of the device, where R is the channel resistance of the FET and C is the shunt capacitance.

One of the solutions to the problem caused by the RC time is to employ a reflectometry technique in which a resonant circuit composed of one inductor and one capacitor is connected to the transistor.[21] This technique expands the bandwidth of the detectable signal frequency and enables single-electron transistors,[7,22–25] quantum point contacts,[26] and Si FETs[27] to detect single electrons with high speed. The basic mechanism of reflectometry is analogous to heterodyne detection commonly used for radio frequency (RF) signals and can be applied to Si FETs at room temperature,[27] which holds promise for expanding the applications of reflectometry. However, detecting a signal of several hundred megahertz is still challenging because the frequency range of a detectable signal is given roughly by the resonance frequency divided by the quality factor of the resonant circuit. Since better charge sensitivity requires a higher quality factor, an increase in the resonance frequency is needed to achieve both faster sensing and higher charge sensitivity at the same time. For example, to detect a signal of several hundred megahertz, the resonance frequency must be about 10 GHz or higher even when a relatively small quality factor of 30 is obtained, as in our device for detecting single electrons.[27]

Here, we report a method for increasing the detectable signal frequency in reflectometry operation of a FET charge sensor. Two resonant circuits connected to the FET, resulting in two resonance frequencies in which RF signals can be driven for the reflectometry, which enables charge sensitivity with single-electron resolution,

Published under an exclusive license by AIP Publishing

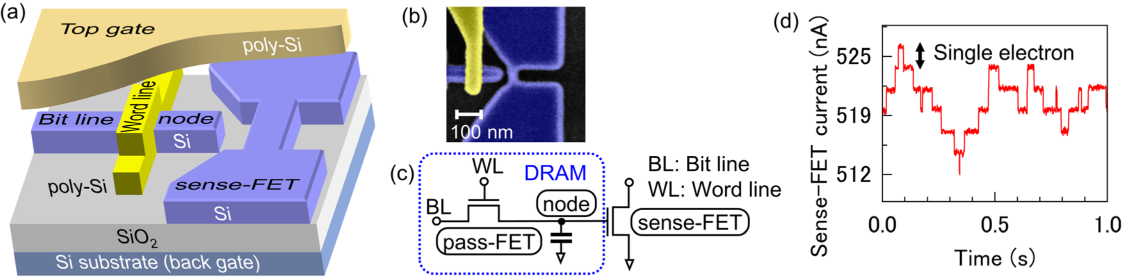

FIG. 1. (a) Bird's-eye view of the device. A top gate covers the entire area. The width and length of the sense-FET channel are estimated to be 10 and 100 nm, respectively. The width of the nanowire channel, or bit line (BL), of the pass-FET is 10 nm. The length of the gate, or word line (WL), of the pass-FET is 15 nm. The gap between the node and sense-FET channel is 50 nm. Details of the fabrication are described in Ref. 27. (b) False scanning electron microscope image without the top gate. (c) Equivalent circuit. In (b) and (c), the top gate is not shown here for simplicity. (d) Real-time detection of a single electron entering and leaving the node. Voltages applied to the top gate, WL, BL, and drain of the sense-FET are 2, −2.35, −1, and 0.1 V, respectively. Measurements are performed with an Agilent 4156C at room temperature. (a) and (b) are reproduced with permission from Nishiguchi *et al.*, Appl. Phys. Lett. **92**, 062105 (2008). Copyright 2008 AIP Publishing. Nishiguchi *et al.*, Appl. Phys. Lett. **98**, 193502 (2011). Copyright 2011 AIP Publishing. Reproduced with permission from Nishiguchi *et al.*, Appl. Phys. Lett. **103**, 143102 (2013). Copyright 2013 AIP Publishing.

3×10^{-3} $e/\mathrm{Hz}^{0.5}$, at 200 MHz signal frequencies. The achievement of this sensitivity, together with readout frequency, is the record at room temperature as far as we know. It should be also noted that our proposal using the two resonant circuits could be adaptable to other devices driven by the reflectometry. Also, since the frequency of the detected signal changes from experiments to experiments, we propose a simple adjustment of sensing characteristics by using a variable capacitor that constitutes the resonant circuits.

To demonstrate the reflectometry, we used a charge sensor based on a 10-nm-channel Si FET (hereafter referred to as the sense-FET) integrated with random access memory (DRAM) as shown in Fig. 1. The FET of the DRAM (hereafter referred to as the pass-FET) uses a gate or word line (WL) to control electron motion between the node and bit line (BL). When the node is completely filled with about 100 electrons in equilibrium, single electrons go and back between the BL and node. This single-electron motion is monitored in real time as discrete changes in current flowing through the sense-FET, dI_{electron}, as shown in Fig. 1(d), because the node functions as a gate of the sense-FET [Fig. 1(c)]. This dI_{electron} is given by the transconductance of the sense-FET multiplied by the variation of the node's voltage caused by a single-electron charging of the channel.[28] On the other hand, when the pass-FET opens completely, the voltage at the node is equal to that at the BL. Therefore, when the pass-FET opens, the change in the BL voltage, which in turn modifies the sense-FET's current by dI_{electron}, can be used as a reference voltage corresponding to that of a single electron. This reference voltage, 8.9 mV, is used for estimating the charge sensitivity in this work because, unlike electrons, the BL voltage is arbitrarily controllable.

Figure 2(a) shows schematics of the reflectometry measurement, in which double resonant circuits are connected to the sense-FET. The double resonant circuits are composed of two inductors with L of 431 nH, a stray capacitor with C_{Stray} of 5.2 pF originating mainly from the wiring of the sense-FET and circuits, and a variable capacitor, C_{Var}. A carrier signal is applied to the sense-FET via the double resonant circuits, and the reflected signal is monitored. Figure 2(b) shows the reflection coefficient (S_{11}) characteristics of the sense-FET combined with the double resonant circuits. Two sharp dips appear at lower and higher resonance frequencies, $f_{\mathrm{reso\text{-}L}}$ and $f_{\mathrm{reso\text{-}H}}$, of 72 and 268 MHz, respectively, due to the double resonant circuits. These two resonance frequencies are given roughly by the following simplified equations:

$$f_{\mathrm{reso-L}} = \frac{1}{2\pi}\sqrt{\frac{2C_{\mathrm{Stray}} + C_{\mathrm{Var}} - \sqrt{4C_{\mathrm{Stray}}{}^2 + C_{\mathrm{Var}}{}^2}}{2LC_{\mathrm{Stray}}C_{\mathrm{Var}}}}, \qquad (1)$$

$$f_{\mathrm{reso-H}} = \frac{1}{2\pi}\sqrt{\frac{2C_{\mathrm{Stray}} + C_{\mathrm{Var}} + \sqrt{4C_{\mathrm{Stray}}{}^2 + C_{\mathrm{Var}}{}^2}}{2LC_{\mathrm{Stray}}C_{\mathrm{Var}}}}. \qquad (2)$$

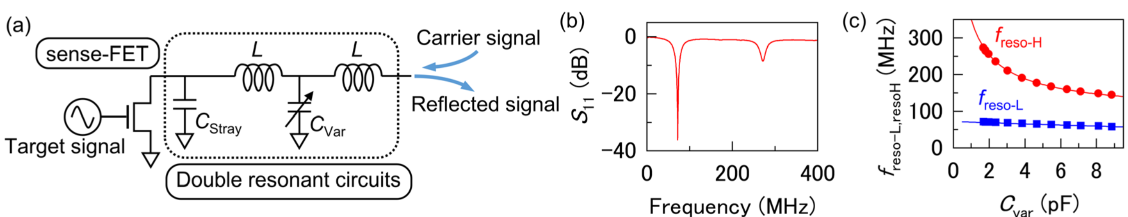

FIG. 2. (a) Schematics of reflectometry measurements. For simplicity, the DRAM is not shown here. The pass-FET is turned on by the WL, and the node is electrically connected to the BL, to which a target signal is applied. Stray capacitance C_{Stray} originating from wiring of the sense-FET and circuits is evaluated to be 5.2 pF from reflection coefficient S_{11} characteristics. C_{Var} is a variable capacitor (Johanson Manufacturing 5201). An inductance L is 431 nH, Coilcraft 2929SQ. (b) S_{11} characteristics. C_{Var} is 1.68 pF. $f_{\mathrm{reso\text{-}L}}$ and $f_{\mathrm{reso\text{-}H}}$ are defined as lower and higher resonance frequencies, respectively. The characteristics are measured by a vector network analyzer (Rohde & Schwarz ZNB). Voltages applied to the top gate, WL, and BL are 2, 2, and 0 V, respectively. (c) Change in $f_{\mathrm{reso\text{-}L}}$ and $f_{\mathrm{reso\text{-}H}}$ as a function of C_{Var}. Closed marks are experimental results. The solid lines are curves fitted to the experimental results with Eqs. (1) and (2) in the main text.

Published under an exclusive license by AIP Publishing

As shown in Fig. 2(c), these equations can reproduce the experimental results obtained when the resonance frequencies are tuned by C_{Var}, which means that the simplified equations can be used to estimate the resonance frequencies.

Figure 3(a) shows the detection of a signal representing 50 electrons by the reflectometry technique. The carrier signal, whose frequency $f_{carrier}$ is close to $f_{reso\text{-}L}$, is applied to the sense-FET combined with the double resonant circuits via a directional coupler [see Fig. 2(a)]. The power of the carrier signal should be as large as possible for better charge sensitivity, and it was adjusted to be 10 dBm in this demonstration. This power is the empirical upper limit that does not damage the sense-FET: when the power becomes larger, hot electrons are generated in the channel[29] and then sometimes increase background noise. In addition, since the large power heats the FET's channel up,[30] its increased temperature might increase the background noise. On the other hand, other devices used for reflectometry, including single-electron transistors and quantum point contacts, must be driven by much smaller power, e.g., -42 dBm or smaller, due to their operating principles. Therefore, the FET has a significant advantage in terms of charge sensitivity. By opening the pass-FET and connecting the BL electrically to the node, an RF target signal to detect, whose frequency is f_{target}, is applied to the BL, i.e., the gate of the sense-FET, as shown in Fig. 2(a). The root mean square voltage of the target signal, 445 mV ($=8.9\,\text{mV} \times 50$), then corresponds to the BL voltage and changes the sense-FET's current by $50 \times dI_{electron}$, which means that the target signal represents 50 electrons. When the frequency spectrum of the reflected signal is monitored by a spectrum analyzer, two peaks appear at either side of the main signal peak at $f_{carrier}$ [Fig. 3(a)]. The side peaks arise from the mixing of the carrier and target signals applied to the sense-FET, with the difference being f_{target}. Thus, in Fig. 3(a), the side peaks at 62 and 82 MHz represent the detection of a 50-electron signal at f_{target} of 10 MHz.

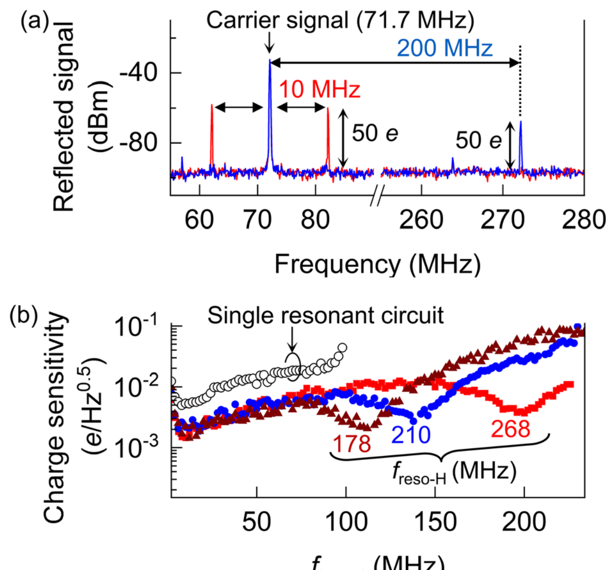

FIG. 3. (a) Detection of the target signal with the reflectometry technique. Frequencies of the target signal are 10 (red) and 200 MHz (blue). The frequency and power of the carrier signal are 71.7 MHz and 10 dBm. $f_{reso\text{-}L}$ and $f_{reso\text{-}H}$ are 72 and 268 MHz. The resolution bandwidth of the spectrum analyzer is 100 kHz. The carrier signal is applied through a coupler, and the reflected signal is monitored with a spectrum analyzer (Rohde & Schwarz FSL). The signal generator for the carrier and target signals is a Rohde & Schwarz SMB 100A. (b) Charge sensitivity characteristics as a function of f_{target} when $f_{reso\text{-}L}$ and $f_{reso\text{-}H}$ are tuned by C_{Var}. The characteristics when a single resonant circuit composed of one inductor and C_{stray} is connected to the sense-FET are also shown. In (a) and (b), L and C_{stray} are the same as the ones in Fig. 2. The voltage applied to the top gate and word line is 2 V.

In reflectometry, frequencies of the main and side peaks must be within the frequency range showing a dip in the S_{11} characteristics. This is because all the signals need to be injected into the resonant circuit near the resonance condition, which determines the range of the detectable f_{target}. In this manner, the range of the detectable f_{target} estimated from the full width at half minimum of the S_{11} characteristics around $f_{reso\text{-}L}$ is about 26.6 MHz [see Fig. 2(b)], which is confirmed by the appearance of the side peaks originating from f_{target} of 10 MHz, as shown in Fig. 3(a). On the other hand, since the double resonant circuits have two resonance conditions as shown in Fig. 2(b), a side peak can also appear around $f_{reso\text{-}H}$, and the target signal at f_{target} of 200 MHz can be monitored as this side peak, as shown in Fig. 3(a).

Figure 3(b) shows the charge-sensitivity characteristics as a function of f_{target} when the resonance frequencies are tuned by C_{Var}. The charge sensitivity, namely, the minimum detectable charge in a frequency range of 1 Hz, is given by $50\ e/(2 \times \text{RBW})^{-0.5}10^{-(\text{SNR}/20)}$, where the factor of 50 accounts for the target signal representing 50 electrons as described above. The factor of 2 accounts for the power collected from both side bands, RBW is the resolution bandwidth of 100 kHz of the spectrum analyzer configured during the measurements, and SNR is the signal-to-noise ratio of the side peak. We achieve the best charge sensitivity of $\sim 2 \times 10^{-3}\ e/\text{Hz}^{0.5}$ at 10 MHz. When f_{target} is lower than 8 MHz, the charge sensitivity becomes worse because the noise floor near f_{target} is higher than for frequencies further than 8 MHz away from it. Since this higher noise near f_{target} appeared even when the sense-FET was disconnected, it could arise from transmission characteristics of the double resonators. When f_{target} is increased from 8 MHz, the charge sensitivity gradually degrades because $f_{target} + f_{carrier}$ corresponding to the frequency of the side peak moves away from $f_{reso\text{-}L}$ for the resonance condition. Then, the charge sensitivity recovers at around $f_{reso\text{-}H} - f_{carrier}$ because $f_{target} + f_{carrier}$ approaches $f_{reso\text{-}H}$ for the other resonance condition, followed by a degradation again. Additionally, by modulating S_{11} characteristics using C_{Var} as shown in Fig. 2(c), the f_{target} dependence of the charge sensitivity is modulated, and the sensitivity reaches $3 \times 10^{-3}\ e/\text{Hz}^{0.5}$ at 200 MHz. This modulation of the charge sensitivity is useful for detecting a signal from an object that oscillates in a narrow frequency bandwidth, such as in a NEMS, so that the frequency giving good charge sensitivity can be adjusted to the target signal.

It must also be pointed out that the double resonators improve the charge sensitivity in the frequency range higher than 100 MHz, where the charge sensitivity of the single resonator is not good enough for single-electron detection as shown by open circles in Fig. 3(b). The possible reason the charge sensitivity of the double resonant circuits is better than that of the single resonant circuit even at frequencies lower than 100 MHz is that channel resistance of the FET is closer to that for impedance-matching condition of the double resonant circuits than that of the single resonant circuit.

The charge sensitivity can be further improved by using an amplifier. The noise in the sense-FET at high frequency is dominated

Published under an exclusive license by AIP Publishing

by thermal noise, which is given by $-174 + 10\log(\text{RBW}) = -124$ dBm at room temperature and, thus, buried in the noise floor (-95 dBm) of the spectrum analyzer. Therefore, there is still a margin of 29 dB for further improvement of the charge sensitivity by using an amplifier. When an amplifier (Mini Circuit ZFL-500LN+) with gain of 28 dB was connected to the double resonators combined with the sense-FET, the noise floor was -88 dBm. Therefore, the signal-to-noise ratio with consideration of the background noise and amplifier gain would be estimated to be 21 [$= 28 - (-88 + 95)$] dB and, thus, the charge sensitivity would be improved to 1.8×10^{-4} and 2.7×10^{-4} $e/\text{Hz}^{0.5}$ at 10 and 200 MHz, respectively. The careful choice of a low-noise preamplifier and large-gain amplifier allows further improvement of charge sensitivity.

To improve the performance further, optimization of the double resonant circuit is needed. Optimal charge sensitivity can be achieved when the sense-FET is impedance-matched with the double resonant circuits. As shown in Fig. 2(b), the minimum S_{11} is larger than -40, which means that there is a window to adjust the impedance matching for better sensitivity. On the other hand, as shown in Fig. 3(b), while the charge-sensitivity characteristics can be modulated by C_{Var}, the charge sensitivity at which the f_{target} dependence of the charge sensitivity shows a dip structure at higher than 100 MHz degrades with a reduction in C_{Var}. This means there is a trade-off between detectable f_{target} and charge sensitivity. One way to mitigate this trade-off would be to reduce C_{stray} to improve the charge sensitivity. The channel resistance of the FET varies by a few orders of magnitude because the top gate adjusts the channel resistance and potential energy of the node so that good charge sensitivity of the FET together with high controllability of single electrons by using the word line can be achieved. The reduction in C_{stray} could make the impedance matching for such widely varying channel resistance of the FET.

In conclusion, we demonstrated reflectometry of FET charge sensors using double resonant circuits. Due to their double resonance characteristics, the detectable frequency of the signal to detect can be extended to 200 MHz with a high charge sensitivity of 3×10^{-3} $e/\text{Hz}^{0.5}$. There is still room to improve this sensitivity by using an amplifier and optimizing the circuits. When future state-of-the-art technologies for high-performance FETs, e.g., subnanometer-node FETs composed of Si, graphene, and/or carbon nanotubes, are able to detect single electrons at intentionally high speed, the reflectometry would boost sensing speed further.

AUTHOR DECLARATIONS

Conflict of Interest

The authors have no conflicts to disclose.

Author Contributions

Katsuhiko Nishiguchi: Conceptualization (equal); Data curation (lead); Formal analysis (lead); Investigation (lead); Methodology (lead); Validation (lead); Visualization (lead); Writing – original draft (lead); Writing – review & editing (lead). **Hiroshi Yamaguchi:** Project administration (equal); Writing – review & editing (equal). **Akira Fujiwara:** Project administration (equal); Writing – review & editing (equal). **Herre S. J. van der Zant:** Project administration (equal); Writing – review & editing (equal). **Gary Alexander Steele:** Conceptualization (lead); Formal analysis (equal); Investigation (equal); Methodology (equal); Project administration (lead); Supervision (lead); Writing – review & editing (equal).

DATA AVAILABILITY

The data that support the findings of this study are openly available in Zenodo at https://doi.org/10.5281/zenodo.7431564.

REFERENCES

[1] K. Nishiguchi, Y. Ono, A. Fujiwara, H. Inokawa, and Y. Takahashi, Appl. Phys. Lett. **92**, 062105 (2008).
[2] K. Nishiguchi and A. Fujiwara, Jpn. J. Appl. Phys., Part 1 **50**, 06GF04 (2011).
[3] J. Hahm and C. M. Lieber, Nano Lett. **4**, 51 (2004).
[4] A. Fujiwara and T. Takahashi, Nature **410**, 560 (2001).
[5] R. G. Knobel and A. N. Cleland, Nature **424**, 291 (2003).
[6] A. N. Korotkov, Phys. Rev. B **60**, 5737 (1999).
[7] W. Lu, Z. Ji, L. Pfeiffer, K. West, and A. Rimberg, Nature **423**, 422–425 (2003).
[8] R. Schleser, E. Ruh, T. Ihn, and K. Ensslin, Appl. Phys. Lett. **85**, 2005 (2004).
[9] J. M. Elzerman, R. Hanson, L. H. Willems van Beveren, B. Witkamp, M. K. Vandersypen, and L. P. Kouwenhoven, Nature **430**, 431–435 (2004).
[10] T. Sagawa and M. Ueda, Phys. Rev. Lett. **102**, 250602 (2009).
[11] C. H. Bennett, Int. J. Theor. Phys. **21**, 905 (1982).
[12] J. Koski, V. Maisi, J. Pekola, and D. Averin, Proc. Natl. Acad. Sci. U. S. A. **111**(38), 13786 (2014).
[13] J. Koski, V. Maisi, T. Sagawa, and J. Pekola, Phys. Rev. Lett. **113**, 030601 (2014).
[14] J. Koski, A. Kutvonen, I. Khaymovich, T. Ala-Nissila, and J. Pekola, Phys. Rev. Lett. **115**, 260602 (2015).
[15] K. Chida, K. Nishiguchi, G. Yamahata, H. Tanaka, and A. Fujiwara, Appl. Phys. Lett. **107**, 073110 (2015).
[16] K. Chida, S. Desai, K. Nishiguchi, and A. Fujiwara, Nat. Commun. **8**, 15310 (2017).
[17] Y. T. Yang, C. Callegari, X. L. Feng, K. L. Ekinci, and M. L. Roukes, Nano Lett. **6**, 583 (2006).
[18] J. Chast, A. Eichler, J. Moser, G. Ceballos, R. Rurali, and A. Bachtold, Nat. Nanotechnol. **7**, 301 (2012).
[19] A. D. O'Connell, M. Hofheinz, M. Ansmann, R. C. Bialczak, M. Lenander, L. Lucero, M. Neeley, D. Sank, H. Wang, M. Weides, J. Wenner, J. M. Martinis, and A. N. Cleland, Nature **464**, 697 (2010).
[20] M. H. Devoret and R. J. Schoelkopf, Nature **406**, 1039 (2000).
[21] R. J. Schoelkopf, P. Wahlgren, A. A. Kozhevnikov, P. Delsing, and D. E. Prober, Science **280**, 1238 (1998).
[22] T. Fujisawa and Y. Hirayama, Appl. Phys. Lett. **77**, 543 (2000).
[23] A. Aassime, G. Johansson, G. Wendin, R. J. Schoelkopf, and P. Delsing, Phys. Rev. Lett. **86**, 3376 (2001).
[24] M. Manoharan, Y. Tsuchiya, S. Oda, and H. Mizuta, Nano Lett. **8**, 4648 (2008).
[25] L. G. Lechner, D. Wu, R. Danneau, S. E. Andersen, and P. Hakonen, J. Appl. Phys. **107**, 084316 (2010).
[26] D. J. Reilly, C. M. Marcus, M. P. Hanson, and A. C. Gossard, Appl. Phys. Lett. **91**, 162101 (2007).
[27] K. Nishiguchi, H. Yamaguchi, A. Fujiwara, H. S. J. Zant, and G. A. Steele, Appl. Phys. Lett. **103**, 143102 (2013).
[28] K. Nishiguchi, C. Koechlin, Y. Ono, A. Fujiwara, H. Inokawa, and H. Yamaguchi, Jpn. J. Appl. Phys., Part 1 **47**, 8305 (2008).
[29] K. Nishiguchi and A. Fujiwara, Appl. Phys. Express **5**, 085002 (2012).
[30] K. Chida, A. Fujiwara, and K. Nishiguchi, Appl. Phys. Lett. **121**, 183501 (2022).

Published under an exclusive license by AIP Publishing